

Direct atomic-orbital-based time-dependent Hartree–Fock calculations of frequency-dependent polarizabilities

Martin Feyereisen, Jeff Nichols,^{a)} Jens Oddershede,^{b)} and Jack Simons
Chemistry Department, University of Utah, Salt Lake City, Utah 84112

(Received 27 September 1991; accepted 13 November 1991)

We have formulated and implemented a direct atomic integral driven method for the calculation of frequency-dependent response properties at the self-consistent-field level. By avoiding the integral transformation step, as well as the storing and retrieving of atomic-orbital-based integrals, we are able to use large basis sets. The practicality of the approach is illustrated and calibrated by performing a series of calculations on cyclopropanone employing up to 232 basis orbitals. We examined the scaling of the dipole polarizability (α) with the size of the system for paranitroaniline and its dimer. Except for a small positive enhancement of the component along the molecular axis, we find little effect of size on α for this system. However, if the –NN– linkage of the dimer is replaced by a –CC– linkage, thus more effectively extending the π -orbital conjugation by making the dimer planar, we find a large, frequency-dependent increase in the polarizability relative to twice that of the monomer (factors varying from 3 to 18, depending on frequency). This makes the –CC– linked polymer a potential candidate for achieving nonlinear chain length dependence of properties that depend on α .

I. INTRODUCTION

Dielectric properties of materials are determined by the polarization of the medium. This macroscopic property is given, for example, by the Clausius–Mossotti relation, in terms of the polarizability tensors $\alpha(E)$ of the individual molecules. It is important to emphasize that $\alpha(E)$ is a frequency-dependent tensorial property. Therefore, when devising computational schemes for evaluating $\alpha(E)$, it is wise to consider methods which (i) can treat all six components of this tensor in a manner whose effort is not 6 times the effort to compute one component, and (ii) can properly handle the frequency dependence for a wide range of energies. In particular, a method that can treat both the frequency-dependent and frequency-independent polarizability with equal accuracy is to be preferred. Although these requirements may seem obvious, they do not characterize the so-called ‘finite field’ methods¹ that are widely used to evaluate molecular polarizabilities.²

In this work, we advocate the use of response function methods,^{3–5} which are often termed polarization propagator methods, because they possess the advantageous properties⁶ outlined earlier. In addition to yielding the polarizability $\alpha(E)$, these methods also allow one to extract electronic excitation energies. The accuracy of these energies compared to experimental data provides a valuable measure of the accuracy of the computed $\alpha(E)$.

From the relatively few *ab initio* calculated frequency-dependent polarizability results^{7–11} that are available at various levels of electron correlation, it appears that $\alpha(E)$ can be well represented at the self-consistent-field (SCF) level of treatment if the electronic state of the system is reasonably

noncorrelated (e.g., as for a closed-shell molecule or atom with no low-energy excited orbitals) and the energy E is not too close to an electronic resonance (i.e., excitation energy) of the system. Close to such resonances, first-order methods do not provide an accurate representation of $\alpha(E)$. Therefore, it is important to have *a priori* knowledge of the resonance positions. Methods such as those used here are capable of providing this information from the eigenspectrum of the response matrix described later.

The treatment in which the electronic state, whose $\alpha(E)$ is to be computed, is treated at the SCF level and response function theory is used to generate $\alpha(E)$, is known as the time-dependent Hartree–Fock (TDHF) or random-phase approximation (RPA). Although the treatment of $\alpha(E)$ for closed-shell species far from electronic excitation resonances may be carried out within the TDHF level, choosing an atomic-orbital basis set for such calculations is far from trivial. It has been found by many workers that reasonably accurate polarizability calculations requires the use of large, flexible, basis sets with diffuse functions and higher angular momentum functions. More than 100 basis functions may be required even for a ‘small’ molecule such as the cyclopropanone system examined here. Because the response theories’ analytical expressions for $\alpha(E)$ are given in terms of SCF orbital energies and two-electron integrals among the SCF molecular orbitals (MO’s), the very time consuming two-electron integral transformation step that plagues most electronic structure calculations has limited finite-field and TDHF calculations of $\alpha(E)$ to small atoms and molecules.

In the present work, we demonstrate how to avoid the integral transformation step within the framework of the TDHF approximation. As a result, we are able to use the DISCO (Ref. 12) package to evaluate two-electron integrals over atomic orbitals (AO’s) and to compute, ‘on the fly’ and without major data storage needs, the contributions of

^{a)} Also at: Utah Supercomputer Institute/IBM Corporation Partnership, Salt Lake City, Utah 84112.

^{b)} Permanent address: Department of Chemistry, Odense University, Odense, Denmark.

each such integral to the matrices that are required by the TDHF procedure. No MO-based integrals are needed, and the AO-based integrals can be discarded as soon as their contributions are evaluated.

Much experience with direct AO-based SCF calculations indicates that the number of nonzero two-electron integrals within conventional AO bases of M orbitals varies as approximately $M^{2.3}$ for large systems. Spatial separation of orbitals on distant atoms results in this reduction from the expected M^4 factor; for large bases and small molecules in which internuclear separations are not large, a dependence closer to M^4 is expected. In either event, the AO-based procedure demonstrated here uses CPU time that varies considerably less strongly than the integral transformation step mentioned earlier, which scales as M^5 . Moreover, because the AO-based integrals do not have to be stored on disk, this method permits work stations having modest amounts of memory to be used to examine much larger species with larger AO basis sets.

To demonstrate the implementation advocated here and to examine potential nonadditivity of $\alpha(E)$ for highly delocalized π -orbital networks, we calculate $\alpha(E)$ for the following.

(i) Cyclopropanone using a series of basis sets containing up to 232 AO's. These calculations allowed us to choose a modestly large basis set that is capable of reproducing the polarizability at the SCF level of theory within $\pm 10\%$ of the values obtained in our largest basis. The compromise basis, which contains 106 Gaussian functions, is labeled $\{2P\}$ in Table I where this and other bases are described and their energies, dipole moments, and polarizabilities given. This basis calibration then allowed us to move on to examine larger molecules.

(ii) The *p*-nitroaniline (pNA) monomer (with bases having up to 272 contracted AO's) and dimer (with up to 294 AO's). The goals of this study were to demonstrate the computational power of the method and to look for possible nonlinearities in the computed values of $\alpha(E)$ as functions of the number of atoms (or electrons) in the system and of energy E .

(iii) A "dimer" molecule formed by linking nitro-

benzene and aniline via a $-\text{CC}-$ linkage to form $\text{O}_2\text{N}-\text{C}_6\text{H}_4-\text{CC}-\text{C}_6\text{H}_4-\text{NH}_2$ using the same bases containing up to 294 AO's. This species is viewed as related to the dimer $\text{O}_2\text{N}-\text{C}_6\text{H}_4-\text{NN}-\text{C}_6\text{H}_4-\text{NH}_2$ of pNA in which the $-\text{NN}-$ linkage is replaced by the $-\text{CC}-$ linkage. Replacing $-\text{NN}-$ by $-\text{CC}-$ was explored because the $-\text{NN}-$ moiety "breaks" the π delocalization between the phenyl rings. In contrast, the $-\text{CC}-$ linkage allows the two rings to retain conjugation, and thus may be expected to give rise to larger in-plane π delocalization and, hence, a larger polarizability component along the long axis of the dimer.

II. FORMULATION OF THE WORKING EQUATIONS

A. Response formulation of polarizability

The *ab initio* calculation of frequency-independent and frequency-dependent polarizabilities of atoms and molecules, α and $\alpha(E)$, can be accomplished via a response function theory. Such approaches express the nine Cartesian components of the tensor $\alpha(E)$ in terms of (i) matrix elements, within a space to be detailed later, of the three Cartesian component electric dipole vector operator \mathbf{r} with elements $\{r_{ma}\}$ and (ii) elements within this same space of two second rank matrices \mathbf{A} and \mathbf{B} whose elements are denoted as $A_{ma,nb}$ and $B_{ma,nb}$. The expression for $\alpha(E)$ is usually written as³

$$\alpha(E) = -2(\mathbf{r} - \mathbf{r}) \begin{pmatrix} E - A & -B^* \\ -B & -E - A^* \end{pmatrix}^{-1} \begin{pmatrix} \mathbf{r} \\ -\mathbf{r} \end{pmatrix}.$$

B. The TDHF approximation

Within the most elementary response function theory known as the time-dependent Hartree-Fock or random-phase-approximation model, the space within which the r_{ma} , $A_{ma,nb}$, and $B_{ma,nb}$ are evaluated is called the space of particle-hole excitations. Within such a theory, the electronic state of the system whose polarizability is sought is treated at the Hartree-Fock self-consistent-field single Slater determinant wave-function level:

$$\Psi = |\phi_1(1)\phi_2(2)\cdots\phi_a(a)\cdots\phi_b(b)\cdots\phi_N(N)|.$$

Here the $\{\phi_a\}$ denote the set of N SCF spin orbitals (orbitals

TABLE I. Energies, dipole moments, and polarizabilities (all numbers given in atomic units) for cyclopropanone within different bases.

Basis	Energy	μ_z	α_{xx}	α_{yy}	α_{zz}	α_{av} ^a
6-31 G** ^b	-189.536	1.873	31.37	13.30	36.54	27.07
KPD ^c	-189.481	1.972	33.89	20.48	41.35	31.91
0P ^d	-188.573	1.735	32.68	14.99	38.26	28.64
1P ^e	-189.128	1.968	32.32	18.92	41.51	31.25
2P ^f	-189.167	2.015	34.79	22.97	42.93	33.56
4P* ^g	-189.610	1.958	35.06	23.03	42.72	33.60

^a $\alpha_{av} = \frac{1}{3}(\alpha_{xx} + \alpha_{yy} + \alpha_{zz})$.

^b (10,4,1/4,1) [3,2,1/2,1], see Ref. 16.

^c (9,5,1/4,1) [3,2,1/2,1], see Ref. 9.

^d (6,3/3) [4,3/3], see text for a complete description.

^e (7,4/4,1) [4,3/3,1], see text for a complete description.

^f (8,5,1/5,1) [5,4,1/4,1], see text for a complete description.

^g (15,10,4/10,4) [7,6,4/6,4], see text for a complete description.

multiplied by α or β) that are occupied in this Slater determinant. The spin orbitals $\{\phi_p\}$ that are not occupied in Ψ are called unoccupied or virtual spin orbitals or "particles." An operator expressed in terms of spin-orbital creation $\{m^\dagger\}$ and destruction $\{a\}$ operators,

$$q_{ma}^\dagger = m^\dagger a,$$

that acts on Ψ to replace the occupied spin-orbital ϕ_a by a virtual spin-orbital ϕ_m , is called a "particle-hole" excitation operator because it creates a hole in a spin orbital that appears in Ψ and a particle in a previously unoccupied spin orbital.

As shown in Ref. 3, within this space of particle-hole operators and taking a single Slater determinant to describe the electronic state of interest, the elements of the \mathbf{r} vector are given as integrals of the dipole operator \mathbf{r} among the unoccupied and occupied SCF molecular orbitals

$$r_{ma} = \langle \phi_m | \mathbf{r} | \phi_a \rangle.$$

In this expression and in all others to follow, the spins of the orbitals are absent because the working expressions obtained in Ref. 3 were derived for closed-shell singlet Ψ 's and for singlet excitation operators q_{ma}^\dagger .

As also shown in Ref. 3, the elements of the A and B arrays are given in terms of orbital energies and two-electron integrals over these same MO's as

$$A_{ma;nb} = \delta_{mn} \delta_{ba} (\epsilon_m - \epsilon_a) - (mn|ba) + 2(ma|bn),$$

$$B_{ma;nb} = (an|bm) - 2(am|bn).$$

Here, Mulliken notation is used for the two-electron integrals

$$(mn|ba) = \int \phi_m^*(1) \phi_n(1) |1/r_{12}| \phi_b^*(2) \phi_a(2) d\tau_1 d\tau_2,$$

and the canonical SCF orbital energies are denoted ϵ_m for virtual orbitals and ϵ_a for occupied orbitals.

III. OVERCOMING DIFFICULTIES WITH TWO-ELECTRON INTEGRALS IN THE MOLECULAR-ORBITAL BASIS AND LARGE PARTICLE-HOLE SPACES

A. The bottleneck of two-electron integrals in the MO basis

One primary difficulty with calculating $\alpha(E)$ in the manner outlined earlier lies in the fact that the \mathbf{A} and \mathbf{B} matrix elements are expressed in terms of two-electron integrals over the canonical MO's. The evaluation of these integrals requires transforming the integrals from the atomic-orbital basis where they are denoted $(ij|kl)$ to the MO basis as, for example,

$$(mn|ba) = \sum_{ijkl} C_{mi} C_{nj} C_{bk} C_{al} (ij|kl),$$

using the linear combination atomic-orbital-molecular-orbital (LCAO-MO) coefficients $\{C_{mi}\}$ that relate the SCF MO's to the original AO's. This integral transformation step requires CPU time proportional to the fifth power of the basis set size, which presents a well known bottleneck to many *ab initio* quantum chemistry calculations.

B. Problems with large particle-hole spaces

Another difficulty lies in computing, storing, and eventually obtaining the inverse of the matrix

$$\begin{pmatrix} E - A & -B^* \\ -B & -E - A^* \end{pmatrix}$$

when its dimension is quite large. The dimension of this matrix is twice the dimension of the particle-hole space. When large AO bases are used, the number of virtual orbitals is quite large. For example, in the calculation whose results are presented here, 294 AO's were employed and gave rise to 62 occupied MO's and 232 virtual MO's, and to a particle-hole space of dimension $232 \times 62 = 14\,384$.

In the present work, we present a reformulation of the above single Slater determinant based, response function formulation of $\alpha(E)$ that does not require the two-electron integrals in the MO basis and does not involve explicit inversion of the large matrix shown earlier. In particular, we compute

$$\begin{pmatrix} E - A & -B^* \\ -B & -E - A^* \end{pmatrix}^{-1} \begin{pmatrix} \mathbf{r} \\ -\mathbf{r} \end{pmatrix}$$

by employing iterative matrix-times-vector methods to solve the set of linear equations

$$\begin{pmatrix} E - A & -B^* \\ -B & -E - A^* \end{pmatrix} \begin{pmatrix} \mathbf{Z} \\ \mathbf{Y} \end{pmatrix} = \begin{pmatrix} \mathbf{r} \\ -\mathbf{r} \end{pmatrix}.$$

Given a converged solution vector $\begin{pmatrix} \mathbf{Z} \\ \mathbf{Y} \end{pmatrix}$, the polarizability $\alpha(E)$ is then computed as

$$\alpha(E) = -2(\mathbf{r} \quad -\mathbf{r}) \begin{pmatrix} \mathbf{Z} \\ \mathbf{Y} \end{pmatrix}.$$

C. Solving large linear equation sets

The implementation of such iterative methods requires that a set of basis vectors $\{\begin{pmatrix} \mathbf{Z}^s \\ \mathbf{Y}^s \end{pmatrix}\}$ be generated, after which the solution vector $\begin{pmatrix} \mathbf{Z} \\ \mathbf{Y} \end{pmatrix}$ is expanded in terms of these basis vectors:

$$\begin{pmatrix} \mathbf{Z} \\ \mathbf{Y} \end{pmatrix} = \sum_s D_s \begin{pmatrix} \mathbf{Z}^s \\ \mathbf{Y}^s \end{pmatrix}.$$

The expansion coefficients $\{D_s\}$ are found by solving the set of 'reduced' linear equations

$$\sum_s (\mathbf{Z}^s \mathbf{Y}^s) \begin{pmatrix} E - A & -B^* \\ -B & -E - A^* \end{pmatrix} \begin{pmatrix} \mathbf{Z}^s \\ \mathbf{Y}^s \end{pmatrix} D_s = (\mathbf{Z}^s \mathbf{Y}^s) \begin{pmatrix} \mathbf{r} \\ -\mathbf{r} \end{pmatrix}$$

that result by substituting the above expansion for $\begin{pmatrix} \mathbf{Z} \\ \mathbf{Y} \end{pmatrix}$ into the full set of linear equations.

Within such methods, successive members

$$\begin{pmatrix} \mathbf{Z}^{s+1} \\ \mathbf{Y}^{s+1} \end{pmatrix}$$

of the vector space are formed in a process that requires multiplying the s th vector in this space $\begin{pmatrix} \mathbf{Z}^s \\ \mathbf{Y}^s \end{pmatrix}$ by the matrix

$$\begin{pmatrix} E - A & -B^* \\ -B & -E - A^* \end{pmatrix} = \mathbf{X}.$$

To begin this process, an initial vector $\begin{pmatrix} \mathbf{Z}^0 \\ \mathbf{Y}^0 \end{pmatrix}$ must be available. In our implementation, this 'seed' vector is formed with elements

$$(E - \epsilon_m + \epsilon_a) \mathbf{Z}_{ma}^0 = \mathbf{r}_{ma},$$

$$(E + \epsilon_m - \epsilon_a) \mathbf{Y}_{ma}^0 = \mathbf{r}_{ma}.$$

That is, the first member of the vector space is formed with \mathbf{Z}^0 and \mathbf{Y}^0 elements obtained by solving the linear equations neglecting all of the two-electron integral contributions.

This ansatz, as well as the algorithm employed to generate subsequent vectors (\mathbf{Z}_n^s) is derived from a linearization of the full linear equation set

$$\mathbf{X} \begin{pmatrix} \mathbf{Z}^s \\ \mathbf{Y}^s \end{pmatrix} = \begin{pmatrix} \mathbf{r} \\ -\mathbf{r} \end{pmatrix},$$

based on decomposing the full \mathbf{X} matrix into its (presumed) dominant diagonal parts,

$$\mathbf{X}_d = \begin{pmatrix} E - \epsilon_m + \epsilon_a & 0 \\ 0 & -E - \epsilon_m + \epsilon_a \end{pmatrix},$$

and its off-diagonal and remaining diagonal parts $\mathbf{X}_{rem} = \mathbf{X} - \mathbf{X}_d$. In this way, one generates a “new” solution vector

$$\begin{pmatrix} \mathbf{Z}_{new} \\ \mathbf{Y}_{new} \end{pmatrix}$$

from a “current” vector (\mathbf{Z}_c^s),

$$\begin{pmatrix} \mathbf{Z}_{new} \\ \mathbf{Y}_{new} \end{pmatrix} = (\mathbf{X}_d)^{-1} \left\{ \begin{pmatrix} \mathbf{r} \\ -\mathbf{r} \end{pmatrix} - \mathbf{X}_{rem} \begin{pmatrix} \mathbf{Z}_c \\ \mathbf{Y}_c \end{pmatrix} \right\}.$$

This new vector is then orthogonalized to the preceding members of the vector space and defined as (\mathbf{Z}_v^1). This orthogonalization process removes the $(\mathbf{X}_d)^{-1} (\mathbf{r}_{-r})$ component of this vector because this component is equal to (\mathbf{Z}_v^0). For this reason, it is possible to use

$$\begin{pmatrix} \mathbf{Z}_{new} \\ \mathbf{Y}_{new} \end{pmatrix} = (\mathbf{X}_d)^{-1} \left\{ -\mathbf{X}_{rem} \begin{pmatrix} \mathbf{Z}_c \\ \mathbf{Y}_c \end{pmatrix} \right\}$$

to generate the new member of the vector space (\mathbf{Z}_v^1).

The two vectors (\mathbf{Z}_v^0) and (\mathbf{Z}_v^1) are then used to form a 2×2

$$(\mathbf{Z}^u \mathbf{Y}^u) \begin{pmatrix} E - A & -B^* \\ -B & -E - A^* \end{pmatrix} \begin{pmatrix} \mathbf{Z}^s \\ \mathbf{Y}^s \end{pmatrix}$$

reduced matrix and two elements of the

$$(\mathbf{Z}^u \mathbf{Y}^u) \begin{pmatrix} \mathbf{r} \\ -\mathbf{r} \end{pmatrix}$$

reduced right-hand side array. The above set of reduced linear equations are then solved to produce $\{D_s\} = \{D_0, D_1\}$ values, which define a new

$$\begin{pmatrix} \mathbf{Z}_c \\ \mathbf{Y}_c \end{pmatrix} = \sum_{s=0,1} D_s \begin{pmatrix} \mathbf{Z}^s \\ \mathbf{Y}^s \end{pmatrix}$$

to be used to generate a new (\mathbf{Z}_{new}^s).

As mentioned earlier in practice, it is found useful to Schmidt orthogonalize newly formed vectors at the s th iteration of this process ($\mathbf{Z}_{v,s+1}^s$) to all earlier vectors $\{(\mathbf{Z}_v^j); j = 1, 2, \dots, s\}$ and to normalize the new vector. As the vector space reaches saturation, it becomes difficult to carry out such orthonormalization; this is a sign that the space is large enough to accurately represent the full solution vector. The

key to an efficient implementation of such an algorithm lies in the method for computing the matrix-vector products $\mathbf{X}_{rem} (\mathbf{Z}^s)$.

D. Expressing the matrix-vector products in terms of AO integrals

The task of forming the aforementioned matrix-times-vector products reduces to forming matrix-vector products of the form $(\mathbf{E} - \mathbf{A})\mathbf{Z} - \mathbf{B}\mathbf{Y}$ and $-\mathbf{B}\mathbf{Z} - (\mathbf{E} + \mathbf{A})\mathbf{Y}$, where these \mathbf{Z} and \mathbf{Y} vectors represent the s th member of the basis vector space discussed earlier. The essence of the approach developed and implemented in this work involves recasting these two products in a manner that does not require access to the two-electron integrals within the MO basis. A similar approach was sketched by Bacskay¹³ and later discussed in more detail by Jensen *et al.*¹⁴ in a more general treatment that does not require the MO's to be of the canonical Hartree-Fock type. Moreover, Bouman *et al.*^{15a} have, in many elegant examples, shown how to solve the large linear equations that arise in the RPA solution in the “direct” approach advocated here (but in the MO rather than the AO basis). However, the only implementation of the procedure is that of Parkinson and Zerner^{15b} within a semiempirical framework where the treatment of the two-electron integrals is considerably simpler. To illustrate how the aforementioned two matrix-vector products can be so rewritten, let us examine the first of these products in further detail.

When written out in terms of the orbital energies and MO-based integrals, and after the MO-based integrals are expressed, using the MO-to-AO transformation defined earlier, the $(\mathbf{E} - \mathbf{A})\mathbf{Z} - \mathbf{B}\mathbf{Y}$ product is seen to be

$$[(\mathbf{E} - \mathbf{A})\mathbf{Z} - \mathbf{B}\mathbf{Y}]_{ma} = (E - \epsilon_m + \epsilon_a) \mathbf{Z}_{ma}$$

$$+ \sum_{nb} \sum_{ijkl} C_{im} C_{jn} C_{kb} C_{la}$$

$$\{[(ij|kl) - 2(il|kj)] \mathbf{Z}_{nb} + [2(li|kj) - (lj|ki)] \mathbf{Y}_{nb}\}.$$

An analogous expression can be written for $[-\mathbf{B}\mathbf{Z} - (\mathbf{E} + \mathbf{A})\mathbf{Y}]_{ma}$; rather than doing so now, the expression for $[(\mathbf{E} - \mathbf{A})\mathbf{Z} - \mathbf{B}\mathbf{Y}]_{ma}$ will be further developed into final working form at which time the corresponding working expression for $[-\mathbf{B}\mathbf{Z} - (\mathbf{E} + \mathbf{A})\mathbf{Y}]_{ma}$ will be given.

Introducing the following definitions

$$\sum_{nb} C_{jn} C_{kb} \mathbf{Z}_{nb} = \mathbf{Z}_{jk}, \quad \sum_{nb} C_{jn} C_{kb} \mathbf{Y}_{nb} = \mathbf{Y}_{jk},$$

$$A_{il,jk} = 2(il|kj) - (ij|kl),$$

$$B_{il,jk} = -2(li|kj) + (lj|ki),$$

allows the aforementioned matrix-vector product to be rewritten as

$$\begin{aligned} [(\mathbf{E} - \mathbf{A})\mathbf{Z} - \mathbf{B}\mathbf{Y}]_{ma} &= (\mathbf{E} - \epsilon_m + \epsilon_a) \mathbf{Z}_{ma} \\ &\quad - \sum_{ijkl} C_{im} C_{la} \{A_{il,jk} \mathbf{Z}_{jk} + B_{il,jk} \mathbf{Y}_{jk}\}. \end{aligned}$$

The corresponding expression for the other matrix-vector product is

$$\begin{aligned} & [-\mathbf{BZ} - (\mathbf{E} + \mathbf{A})\mathbf{Y}]_{ma} \\ & = (-\mathbf{E} - \epsilon_m + \epsilon_a) \mathbf{Y}_{ma} \\ & \quad - \sum_{ijkl} C_{im} C_{la} \{ B_{il,jk} \mathbf{Z}_{jk} + A_{il,jk} \mathbf{Y}_{jk} \}. \end{aligned}$$

IV. COMPUTER IMPLEMENTATION OF WORKING EQUATIONS

The aforementioned expressions allow the two matrix-vector products to be carried out entirely in terms of AO-bases two-electron integrals. In our approach, the following steps are carried out.

(1) Given the solution vector ($\mathbf{Z}_{Y^s}^c$) resulting from solving the reduced linear equations within the space of dimension s , the LCAO-MO coefficients are used to transform the elements of the \mathbf{Z}^m and \mathbf{Y}^m vectors from the MO to the AO basis using

$$\sum_{nb} C_{jn} C_{kb} \mathbf{Z}_{nb}^c = \mathbf{Z}_{jk}^c$$

and

$$\sum_{nb} C_{jn} C_{kb} \mathbf{Y}_{nb}^c = \mathbf{Y}_{jk}^c.$$

This two-indexed transformation requires CPU time proportional to $M^2 N_h + M N_p N_h$, where M is the number of contracted AO's in the basis set, N_p is the number of virtual MO's, and N_h is the number of occupied orbitals. This pair $\{\mathbf{Z}_{jk}^c\}$ and $\{\mathbf{Y}_{jk}^c\}$ of two-indexed arrays (each of dimension M^2) is stored in the computer's main memory.

(2) Two arrays $\{Q_{il}\}$ and $\{P_{il}\}$ are initialized (i.e., their elements are set equal to zero). The DISCO program is then allowed to generate Gaussian AO-based integrals ($ij|kl$) during which contributions to the sums

$$Q_{il} = \sum_{kj} \{ B_{il,jk} \mathbf{Z}_{jk}^c + A_{il,jk} \mathbf{Y}_{jk}^c \}$$

and

$$P_{il} = \sum_{kj} \{ A_{il,jk} \mathbf{Z}_{jk}^c + B_{il,jk} \mathbf{Y}_{jk}^c \}$$

are accumulated. In practice, the index permutational symmetry of the two-electron integrals involving real Gaussian functions (e.g., $(ij|kl) = (ji|kl) = (kl|ij)$) can be exploited to form the Q_{il} and P_{il} arrays in a manner somewhat more efficient than described earlier.

Upon the completion of the AO-integral generation steps, the $\{Q_{il}\}$ and $\{P_{il}\}$ arrays contain the aforementioned sums; the $\{\mathbf{Z}_{jk}^c\}$ and $\{\mathbf{Y}_{jk}^c\}$ arrays can now be discarded to save memory. The AO-based integrals are never stored on disk; their contributions to the $\{Q_{il}\}$ and $\{P_{il}\}$ arrays are accumulated "on the fly" and the integrals are subsequently discarded. This part of the program requires CPU time proportional to $M^{2.3}$ to M^4 since only symmetry-allowed non-zero AO-based integrals must be evaluated.

(3) Once the $\{Q_{il}\}$ and $\{P_{il}\}$ are computed, the sums

$$\sum_{il} C_{im} C_{la} Q_{il} = Q_{ma}$$

and

$$\sum_{il} C_{im} C_{la} P_{il} = P_{ma}$$

are evaluated in CPU times proportional to $M^2 N_h + M N_p N_h$. This completes the steps needed to evaluate the two-electron integral contributions to $\mathbf{X}_{\text{rem}}(\mathbf{Z}^s)$. Keeping in mind that \mathbf{X}_{rem} contains all of the two-electron integrals' contribution to \mathbf{X} , it becomes clear that

$$\mathbf{X}_{\text{rem}} \begin{pmatrix} \mathbf{Z}^s \\ \mathbf{Y}^s \end{pmatrix} = - \begin{pmatrix} \mathbf{P} \\ \mathbf{Q} \end{pmatrix},$$

where the elements of \mathbf{P} and \mathbf{Q} are P_{ma} and Q_{ma} , respectively.

(4) Having formed $\mathbf{X}_{\text{rem}}(\mathbf{Z}^s)$, the algorithm

$$\begin{pmatrix} \mathbf{Z}^{s+1} \\ \mathbf{Y}^{s+1} \end{pmatrix} = (\mathbf{X}_d)^{-1} \left\{ -\mathbf{X}_{\text{rem}} \begin{pmatrix} \mathbf{Z}^s \\ \mathbf{Y}^s \end{pmatrix} \right\}$$

can be used to determine the next member ($\mathbf{Z}_{Y^{s+1}}^{s+1}$) of the vector space. Of course, this vector is then Schmidt orthogonalized to all $\{\mathbf{Z}_{Y^j}^j\}; j = 1, 2, 3, \dots, s\}$. Considering the form of \mathbf{X}_d , it is straightforward to write the elements of ($\mathbf{Z}_{Y^{s+1}}^{s+1}$) as

$$\mathbf{Z}_{ma} = P_{ma} (\mathbf{E} - \epsilon_m + \epsilon_a)^{-1},$$

$$\mathbf{Y}_{ma} = Q_{ma} (-\mathbf{E} - \epsilon_m + \epsilon_a)^{-1}.$$

(5) With a new member of the vector space in hand, the matrix

$$(\mathbf{Z}^u \mathbf{Y}^u) \begin{pmatrix} \mathbf{E} - \mathbf{A} & -\mathbf{B}^* \\ -\mathbf{B} & -\mathbf{E} - \mathbf{A}^* \end{pmatrix} \begin{pmatrix} \mathbf{Z}^s \\ \mathbf{Y}^s \end{pmatrix}$$

can be formed for one higher dimension, as can the

$$(\mathbf{Z}^u \mathbf{Y}^u) \begin{pmatrix} \mathbf{r} \\ -\mathbf{r} \end{pmatrix}$$

array, and the reduced linear equations of one higher dimension can be solved for new $\{D_s\}$ elements. This, in turn, defines a new approximation to the solution vector

$$\begin{pmatrix} \mathbf{Z}^c \\ \mathbf{Y}^c \end{pmatrix} = \sum_{u=0, s+1} D_u \begin{pmatrix} \mathbf{Z}^u \\ \mathbf{Y}^u \end{pmatrix}$$

whose elements \mathbf{Z}_{ma}^c , and \mathbf{Y}_{ma}^c can be used to begin a new iteration.

V. CALCULATIONS AND RESULTS

A. Basis calibration calculations on cyclopropenone

The cyclopropenone (CP) molecule $\text{C}_3\text{H}_2\text{O}$ (see Fig. 1) is used in this work to develop an atomic-orbital basis set for subsequent use on the target paranitroaniline (pNA) molecule and its dimer. CP is thought to be a reasonable "basis calibration" molecule because, like pNA, it contains a delocalized π -orbital network involving heteroatoms. However, because it contains only four "heavy" (i.e., non-hydrogen) atoms, it is possible to explore AO basis sets that are

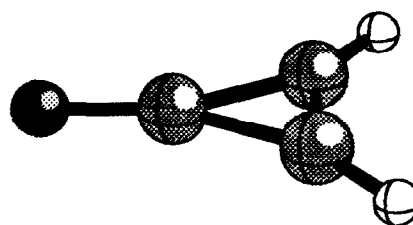


FIG. 1. Cyclopropenone.

TABLE II. Exponent optimization for the $2P$ basis for cyclopropanone (all numbers given in atomic units).

$\zeta(d)$	$\zeta(p)$	Energy	μ_z	α_{xx}	α_{yy}	α_{zz}	α_{av}
0.76	0.76	-189.256	1.932	34.05	19.75	42.41	32.07
0.76	0.60	-189.255	1.932	34.09	19.90	42.46	32.15
0.76	0.50	-189.254	1.932	34.10	20.05	42.49	32.21
0.76	0.40	-189.253	1.932	34.08	20.27	42.50	32.28
0.76	0.30	-189.251	1.932	33.99	20.58	42.48	32.35
0.76	0.20	-189.249	1.929	33.87	20.93	42.33	32.38
0.76	0.10	-189.249	1.929	33.99	20.90	42.18	32.36
0.60	0.20	-189.244	1.930	34.09	21.22	42.39	32.57
0.50	0.20	-189.235	1.931	34.27	21.50	42.49	32.75
0.40	0.20	-189.221	1.935	34.49	21.87	42.65	33.00
0.30	0.20	-189.199	1.953	34.69	22.35	42.88	33.31
0.20	0.20	-189.167	2.015	34.79	22.97	42.93	33.56
0.10	0.20	-189.149	1.993	34.84	22.37	43.67	33.63

large enough to yield $\alpha(E)$ data accurate to within $\pm 10\%$ compared to the SCF limit (i.e., ignoring electron correlation effects). Such basis exploration is carried out in search of an AO basis that is capable of providing a $\pm 10\%$ level description of $\alpha(E)$ that is computationally feasible for use on the pNA monomer and dimer. To obtain a geometry for CP at which to carry out the aforementioned test calculations, we performed a full geometry optimization using an atomic-orbital basis set from Ref. 17 of [6, 3 | 3, 2] quality for non-hydrogen atoms and [3 | 2] quality for the hydrogen atoms. This geometry is available upon request.

In Table I are the results [total SCF energies, dipole moments, the three principal components of the $\alpha(E=0)$ tensor, and $\alpha_{av} = \frac{1}{3}(\alpha_{xx} + \alpha_{yy} + \alpha_{zz})$] for the CP molecule obtained using a series of basis sets. Here, the molecule is situated with its natural dipole moment along the z axis and the π orbitals aligned with the y axis. The first bases, 6–31 G** (Ref. 16) are listed to give an indication of the demands of a basis when computing polarizabilities. While the total energy is quite good for this basis, the dipole moment and polarizabilities are inaccurate due to the lack of diffuse flexibility of the basis. The second basis refers to that used by Karna, Prasad, and Dupuis⁹ who, in their excellent study of the pNA monomer, developed this basis by adding diffuse and polarization functions to a Dunning–Hay (DH) contracted Gaussian basis.

The sixth basis listed (denoted as $4P$), was constructed from a van Duijneveldt¹⁷ (13,8/8) primitive set contracted

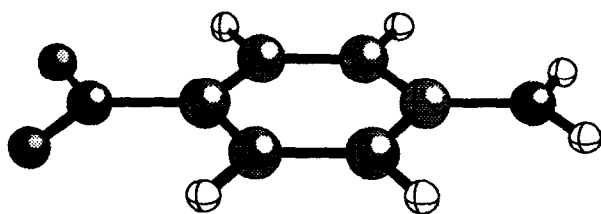
to [2,1/1] using the AO's obtained from a SCF calculation of the neutral atoms. Additionally, the outermost functions were uncontracted, giving the set [5,4/4]. Diffuse functions were added to this set by multiplying the outermost exponents by a factor of 0.4 giving the set [7,6/6]. Four uncontracted polarization functions were added. The exponents for the d functions on the heavy atoms were 3.0, 1.2, 0.48, and 0.192. The exponents for the p functions added to the hydrogens were 1.7, 0.68, 0.272, and 0.1088. The final set used for the calculations was thus (15,10,4/10,4) [7,6,4/6,4].

The fifth basis was derived to reproduce the results of the ($4P$) basis. The set denoted as ($2P$) was obtained from adding a (2,2/2) diffuse set along with a single polarization set to the van Duijneveldt primitive set (6,3/3) and contracting in the same manner described for the ($4P$) set, giving the set (8,5,1/5,1) [5,4,1/4,1]. The polarization exponents were optimized (see Table II), obtaining the values of 0.2 for both the p and d functions.

Table III demonstrates the effects of removing the polarization functions from the ($2P$) and ($4P$) bases on the total energy, dipole moment, and polarizability components of CP. For both bases, the d polarization function on the heavy atoms has a substantially greater effect on the polarizability, particularly in the y direction. Nevertheless, it appears possible to qualitatively predict polarizabilities to $\pm 20\%$ by excluding both the p and d polarization functions from the bases. This could be advantageous for polarizability

TABLE III. Energies, dipole moments, and polarizabilities (all numbers given in atomic units) for cyclopropanone for modified $2P$ and $4P$ bases.

Basis	Energy	μ_z	α_{xx}	α_{yy}	α_{zz}	α_{av}
($2P$)-SP/S	-189.133	1.990	33.17	18.08	43.00	31.42
($2P$)-SP/SP	-189.137	2.000	33.06	19.91	43.10	32.02
($2P$)-SPD/S	-189.164	2.016	34.49	22.97	42.95	33.47
($2P$)-SPD/SP	-189.167	2.015	34.79	22.97	42.93	33.60
($4P$)-SP/S	-189.500	2.022	33.21	18.13	43.08	31.47
($4P$)-SP/SP	-189.513	2.031	33.51	20.22	43.44	32.39
($4P$)-SPD/S	-189.605	1.956	34.98	22.70	42.66	33.45
($4P$)-SPD/SP	-189.610	1.958	35.06	23.03	42.72	33.60

FIG. 2. pNA monomer $O_2N-C_6H_4-NH_2$.

studies of larger systems, where the inclusion of polarization functions would be computationally prohibitive. The third and fourth bases in Table I were constructed for such studies. The set (1P) was obtained by removing the contracted set [1,1,1/1,0] from the (2P) set, giving (7,4/4,1) [4,3/3,1]. The basis (0P) was constructed from the van Duijneveldt (5,2/2) set, adding (1,1/1) diffuse functions, and contracting as before for the set (6,3/3) [4,3/3]. Table I clearly shows that significant reductions in all α components accompany either change in basis, especially when polarization functions are removed from the hydrogen atoms and especially along the out-of-plane y direction. For this reason, the 0P and 1P basis results can not be used as $\pm 10\%$ representations of the SCF limit values. However, it is likely that α values at the 2P basis level for the pNA dimer can be estimated by scaling the 0P basis results (i.e., α_{av}) by ratios obtained for CP α values within the 2P, 1P, and 0P bases; these ratios are 1.00:0.92:0.85, respectively, for the 2P:1P:0P bases.

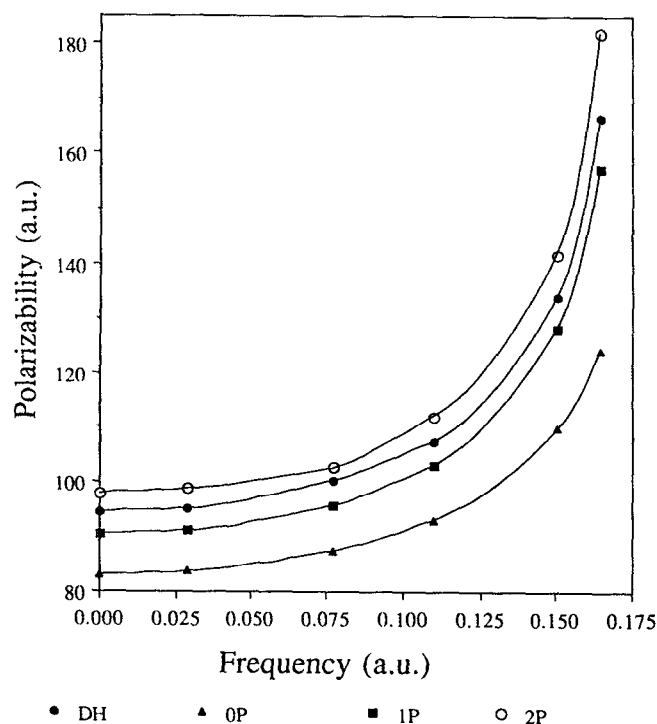


FIG. 3. Frequency-dependant polarizability of pNA for various basis sets.

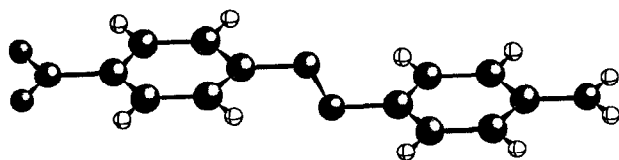
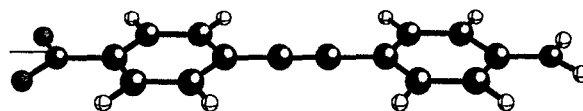
B. The pNA monomer and dimer

The geometry used in all of the pNA calculations was taken from Ref. 9 where its optimization is described. For the following calculations on the pNA dimer as well as on its $-CC-$ linked dimer, we performed full geometry optimiz-

TABLE IV. Energies, dipole moments, and polarizabilities for pNA.

Basis	Freq. ^a	Energy	μ_z	α_{xx}	α_{yy}	α_{zz}	α_{av}
KPD	0.000 000	- 489.127	3.108	91.1	48.7	137.7	92.5
	0.028 838			97.5	48.8	138.6	95.0
	0.077 358			101.2	49.4	150.4	100.3
	0.109 809			105.2	50.1	167.0	107.4
	0.150 380			115.9	51.4	234.9	133.9
	0.164 713			122.0	52.0	325.6	166.5
0P	0.000 000	- 486.750	2.901	90.7	37.0	121.3	83.0
	0.028 838			91.1	37.1	122.5	83.6
	0.077 358			94.1	37.6	130.4	87.4
	0.109 809			98.1	38.1	142.8	93.0
	0.150 380			107.3	39.3	182.6	109.7
	0.164 713			112.6	39.9	219.7	124.1
1P	0.000 000	- 488.208	3.140	94.6	46.3	130.3	90.4
	0.028 838			95.0	46.4	131.7	91.0
	0.077 358			98.3	47.1	141.8	95.7
	0.109 809			102.8	48.0	158.4	103.1
	0.150 380			113.2	49.7	221.7	128.3
	0.164 713			119.4	50.8	301.8	157.3
2P	0.000 000	- 488.281	3.158	98.7	53.6	141.3	97.9
	0.028 838			99.2	53.7	142.8	98.6
	0.077 358			102.6	54.7	153.9	102.6
	0.109 809			107.4	55.8	172.7	112.0
	0.150 380			118.4	58.3	248.8	141.8
	0.164 713			125.0	59.6	360.9	181.8

^aFrequency in atomic units.

FIG. 4. -NN- linked dimer $O_2N-C_6H_4-NN-C_6H_4-NH_2$.FIG. 5. -CC- linked dimer $O_2N-C_6H_4-CC-C_6H_4-NH_2$.

ation using an atomic-orbital basis set from Ref. 17 of [6, 3 | 3, 2] quality for non-hydrogen atoms and [3 | 2] quality for the hydrogen atoms. Our optimized geometries are available upon request.

Having calibrated the quality of the α values obtained within the $2P$, $1P$, and $0P$ bases at this SCF response theory level, we undertook the considerably more challenging task of calculating $\alpha(E)$ for the pNA monomer and dimer. These species contain, respectively, 10 and 18 heavy atoms and 6 and 10 hydrogen atoms. Using the $2P$ basis, these species would require 338 and 602 primitive Gaussian AO's.

The pNA monomer (see Fig. 2) results obtained in this study for $\alpha(E)$, for selected frequencies $h\nu = E$ reported in Ref. 9, are displayed in Table IV and in Fig. 3. The first set of results contained in Table IV are those of Ref. 9; clearly, the AO basis used by these earlier workers is energetically superior to our own. This is due to the sparseness of primitive functions with large exponents needed to accurately describe the cusp of the core orbitals. However, our $2P$ basis produces, as it did for the CP calibration molecule, somewhat larger α values. Our $1P$ and $0P$ bases produce α values that are within $\pm 20\%$, yet systematically smaller than those of our $2P$ basis or those of Ref. 9. The ratios of α_{av} values for the pNA monomer within the $2P:1P:0P$ bases are 1.00:0.91:0.83, which are very nearly the same as the ratios observed for the CP species. Our $2P$ and $1P$ basis results seem to bracket those of Ref. 9 at all frequencies reported in Table IV.

The pNA dimer (see Fig. 4) α values obtained in the $1P$ and $0P$ bases are shown in Table V. Corresponding α values for the $2P$ basis are estimated by multiplying the $1P$ results by the scale factor $1.00/0.91 = 1.10$ observed to hold for the pNA monomer. The results of both the $1P$ and $2P$ bases show slight positive nonadditivity in the α_{zz} (along the long axis of the molecule) principal component of α and negative deviations from additivity in the α_{xx} (the in-plane axis perpendicular to the long axis) and α_{yy} (the out-of-plane axis) components of α . We had expected that α_{zz} for the dimer would be considerably more than twice α_{zz} for the monomer

because of the high degree of π -electron delocalization along the z axis and the presence of low-energy charge transfer (of the type $O_2N-R-NH_2$ to $^-O_2N-R-N^+H_2$) and because simple models predict the polarizability to be proportional to the third power of the length of the system.¹⁸

C. The -CC- linked pNA dimer

After finding that α_{zz} seems to scale nearly linearly with the size of the molecule for the pNA monomer and dimer, we examined the dimer in which the -NN- linkage is replaced by a -CC- linkage (see Fig. 5). The fact that -N=N- involves sp^2 N atoms causes the two phenyl rings linked by this -N=N- group to become noncoplanar. In contrast, the -CC- moiety involves sp hybridized C atoms, as a result of which the two phenyl rings linked through -CC- can remain coplanar. Based on these geometrical considerations, we believed that -CC- linked pNA dimer would have α_{zz} values substantially more than twice that of the pNA monomer.

The results obtained for the -CC- linked pNA dimer are shown in Table VI. Unlike the -NN- linked dimer, the -CC- linked dimer shows a static α_{zz} value that is considerably more than twice (in fact, 2.8 times) that of the monomer. At higher frequencies, this ratio is even larger; at $E = 0.1647$, the ratio is greater than 18. The other two components α_{xx} and α_{yy} of the -CC- linked species are similar to those of the -NN- dimer. It seems, therefore, that the -CC- linked polymers may be better candidates for achieving highly nonlinear (with regard to chain length dependence of molecular properties) behavior of properties that depend on $\alpha(E)$. Of course, the propensity of such chains to stack in a manner that may destroy long-range delocalization of the π orbitals may limit the practicality of such a proposal.

D. CPU time requirements

The IBM 3090vf600 times needed to carry out the TDHF calculations (including all integral evaluation, linear equation solution, etc.), as well as the times needed to obtain converged SCF molecular orbitals for the pNA monomer,

TABLE V. Energies, dipole moments, and static polarizabilities for -NN- linked pNA dimer.

Basis	Energy	μ_z	α_{xx}	α_{yy}	α_{zz}	α_{av}
$0P$	- 823.473	3.068	160.9	76.4	254.6	164.0
$1P$	- 825.906	3.281	166.1	92.1	262.6	173.6
$2P^*$			183	101	288	191

* Estimated using the scaling factor for bases $2P:1P$ as described in the text.

TABLE VI. Energies, dipole moments, and polarizabilities for $-CC-$ linked pNA dimer.

Basis	Freq.	Energy	μ_z	α_{xx}	α_{yy}	α_{zz}	α_{av}
0P	0.000 000	- 790.548	3.435	162.0	70.0	337.9	190.0
	0.028 838			162.8	70.1	342.9	191.9
	0.077 358			168.1	71.0	380.8	206.6
	0.109 809			175.4	72.0	451.6	233.0
	0.150 380			192.4	74.2	897.1	387.9
	0.164 713			202.7	75.3	3994.7	1424.2
1P	0.000 000	- 792.871	3.686	167.1	86.0	350.8	201.3
2P ^a	0.000 000			203	94	461	253

^a Estimated using the scaling factor for bases 2P:1P as described in the text.

and dimers within the 0P, 1P, and 2P bases are given in Table VII. Here, the sizes of the atomic-orbital bases used for each such calculation are also listed.

VI. SUMMARY AND CONCLUSIONS

We have put forth and demonstrated the practicality of a method for direct calculation of frequency-dependent polarizabilities at the SCF level based on the DISCO program. It is AO integral driven so the M^5 integral transformation step is avoided. The method thus scales at worst as M^4 , the time it takes to compute the AO integrals. The rest of the steps in the procedure scale as M^2 .

The method is formulated within the framework of response theory which means that we can evaluate both static and frequency-dependent polarizabilities and that the computational effort of the method does not vary with the number of components of α . This paper thus describes an AO-based time-dependent Hartree-Fock (TDHF) method (often referred to as the random-phase approximation). The TDHF equations are solved using an iterative reduced linear equation¹⁹ technique as described in Sec. III C, thereby circumventing the problem of finding the inverse of a large matrix.

The first step in the application of this method is to

choose a suitable one-electron AO basis set. The cyclopropenone calculations show that for an accuracy of about $\pm 10\%$ in $\alpha(E)$, one needs to include both diffuse and polarization functions in the basis set (the 4P set). One polarization function on each atom is not sufficient (the 2P set) to achieve this accuracy. However, calculations on both cyclopropenone and the pNA monomer show that there seems to be nearly fixed ratios between $\alpha(E)$ computed in the 0P, 1P, and 2P bases. We have thus been able to scale values of $\alpha(E)$ computed in smaller bases to estimate values for larger bases.

We have investigated the variation of $\alpha(E)$ with the size of system in two cases: (i) pNA and its dimer and (ii) a dimer where the $-NN-$ linkage of pNA-pNA is replaced by a $-CC-$ linkage. In case (i) we find only a small positive non-additivity in α for the component along the intermolecular axis and negative deviations for the two other directions. For the $-CC-$ linked dimer, α_{zz} is much larger for the dimer than twice that of the monomer, illustrating the effect of the enhanced conjugation of this planar system relative to the non-planar pNA dimer. This nonlinearity is a strong function of frequency (see, for example, Tables IV and VI).

The essential requirement for the formulation of the AO-driven construction of $\alpha(E)$ as outlined in the present work is that the requisite matrix-times-vector products only involve one two-electron integral at a time and never prod-

TABLE VII. Total time (CPU time in hours for DISCO on an IBM3090vf600) to compute polarizabilities.

Basis	Freq.	pNA	Dimer ($-NN-$)	Dimer ($-CC-$)
0P	0.000 000	1.4 ^a	18.2 ^b	10.6 ^c
	0.028 838	3.0		29.7
	0.164 713	4.0		48.1
1P	0.000 000	4.1 ^d	74.7 ^e	34.8 ^f
	0.028 838	7.2		
	0.164 713	9.3		
2P	0.000 000	23.5 ^g		
	0.028 838	41.5		
	0.164 713	52.9		

^a 148 basis orbitals are used in this calculation.

^b 264 basis orbitals are used in this calculation.

^c 264 basis orbitals are used in this calculation.

^d 166 basis orbitals are used in this calculation.

^e 294 basis orbitals are used in this calculation.

^f 294 basis orbitals are used in this calculation.

^g 272 basis orbitals are used in this calculation.

ucts of two or more two-electron integrals. This requirement is also met for response calculations of frequency-dependent first hyperpolarizabilities β (Refs. 20 and 21), and work on the evaluation of β along the same lines as for α is underway.

ACKNOWLEDGMENTS

J. O. would like to thank the Department of Chemistry, University of Utah for excellent working conditions during his sabbatical during which this work was initiated. This work is supported in part by a grant to J. O. from the Danish Natural Science Research Council (Grant No. 11-9004). Moreover, this work was supported in part by the Office of Naval Research and by the National Science Foundation Grant No. CHE8814765. We also thank the Utah Super-computer Institute for staff and computer resources.

¹ H. D. Cohen and C. C. J. Roothaan, *J. Chem. Phys.* **43**, S34 (1965).

² C. E. Dykstra, *Ab Initio Calculations of the Structures and Properties of Molecules* (Elsevier, Amsterdam, 1988).

³ P. Jørgensen and J. Simons, *Quantum Chemistry: Second Quantization-Based Methods* (Academic, New York, 1981).

⁴ J. Oddershede, P. Jørgensen, and D. L. Yeager, *Comp. Phys. Rep.* **2**, 33 (1989).

⁵ J. Olsen and P. Jørgensen, *J. Chem. Phys.* **82**, 3235 (1985).

⁶ J. Oddershede and J. R. Sabin, *Int. J. Quantum Chem.* **39**, 371 (1991).

⁷ J. E. Rice and N. C. Handy, *J. Chem. Phys.* **94**, 4959 (1991).

⁸ H. Sekino and R. J. Bartlett, *J. Chem. Phys.* **84**, 2726 (1986).

⁹ S. P. Karna, P. N. Prasad, and M. Dupuis, *J. Chem. Phys.* **94**, 1171 (1991).

¹⁰ J. Oddershede and E. N. Svendsen, *Chem. Phys.* **64**, 359 (1982).

¹¹ S. P. A. Sauer, G. H. F. Diercksen, and J. Oddershede, *Int. J. Quantum Chem.* **39**, 667 (1991).

¹² J. Almlöf, K. Faegri, Jr., M. Feyereisen, and K. Korsell, DISCO, a direct SCF and MP2 code.

¹³ G. B. Bacskay, *Aust. J. Phys.* **35**, 639 (1982).

¹⁴ H. J. Aa. Jensen, H. Koch, P. Jørgensen, and J. Olsen, *Chem. Phys.* **119**, 297 (1988).

¹⁵ (a) T. P. Bouman, A. E. Hansen, B. Voigt, and Sten Rettrup, *Int. J. Quantum Chem.* **23**, 595 (1983); (b) W. A. Parkinson and M. C. Zerner, *J. Chem. Phys.* **90**, 5605 (1989).

¹⁶ R. Krishnan, J. S. Binkley, R. Seeger, and J. A. Pople, *J. Chem. Phys.* **71**, 650 (1980).

¹⁷ F. B. van Duijneveldt, IBM Res. RJ 945 (1971).

¹⁸ A. F. Garito, K. D. Singer, and C. C. Teng, in *Nonlinear Optical Properties of Organic and Polymer Materials*, Vol. 1 of the ACS Symposium Series, edited by D. J. Williams (American Chemical Society, Washington, D.C., 1983).

¹⁹ J. A. Pople, R. Krishnan, H. B. Schlegel, and J. S. Binkley, *Int. J. Quantum Chem.* **S13**, 225 (1979).

²⁰ E. Dalgaard, *Phys. Rev. A* **26**, 42 (1982).

²¹ W. A. Parkinson and J. Oddershede, *J. Chem. Phys.* **94**, 7251 (1991).